HIGH-FREQUENCY TECHNIQUES FOR RCS PREDICTION OF PLATE GEOMETRIES

Semiannual Progress Report

Constantine A. Balanis and Lesley A. Polka

August 1, 1990 - January 31, 1991

Department of Electrical Engineering
Telecommunications Research Center
Arizona State University
Tempe, Arizona 85287-7206

Grant No. NAG-1-562
National Aeronautics and Space Administration
Langley Research Center
Hampton, VA 23665

HIGH-FREQUENCY TECHNIQUES FOR RCS PREDICTION OF PLATE GEOMETRIES

Semiannual Progress Report

Constantine A. Balanis and Lesley A. Polka

August 1, 1990 - January 31, 1991

Department of Electrical Engineering
Telecommunications Research Center
Arizona State University
Tempe, Arizona 85287-7206

Grant No. NAG-1-562
National Aeronautics and Space Administration
Langley Research Center
Hampton, VA 23665

ABSTRACT

This report examines several different high-frequency methods for modeling the RCS of plate geometries. The Method of Equivalent Currents and a numerically derived corner diffraction coefficient are used to model the RCS of a rectangular, perfectly conducting plate in nonprincipal planes. The Uniform Theory of Diffraction is used to model the RCS of a rectangular, perfectly conducting plate in principal planes. For the soft polarization case, first-order and slope-diffraction terms are included. For the hard polarization case, up to four orders of diffraction are included. Finally, the Uniform Theory of Diffraction for impedance wedges and the Impedance Boundary Condition are used to model the RCS of a coated, rectangular plate in principal planes. In most of the cases considered, comparisons are made between theoretical and experimental results.

I. INTRODUCTION

Previous reports have detailed high-frequency models for nonprincipal-plane scattering from perfectly conducting plates [1]-[3] and for principal-plane scattering from coated plates [4]. Results from high-frequency models for principal-plane scattering from perfectly conducting plates [4] and dihedral corner reflectors [4] and for coated dihedral corner reflectors [4] have also been presented. These are all important basic geometries serving as building blocks for complicated target geometries. First-order models have yielded excellent results near main lobes, away from grazing incidence angles. For incidence angles away from normal (greater than 60° from normal), the discrepancies in the comparisons of the patterns are due to higher-order diffraction mechanisms, such as interactions between parallel and adjacent sides of the scatterer and corner scattering. Higher-order diffraction mechanisms are not easily modeled using traditional applications of high-frequency techniques, such as the Uniform Theory of Diffraction (UTD) [5] and the Method of Equivalent Currents (MEC) [6]-[9].

Both the UTD and the MEC use the canonical infinite wedge structure to arrive at general models that can be used to approximate the fields scattered by objects that can be represented in a local sense as an infinite wedge. For example, for large side dimensions, a

rectangular plate is modeled as four independent half-planes with no mutual interaction between the edges. The UTD diffraction coefficients are sufficient for two-dimensional scattering problems, such as the scattering from an infinite strip of finite width and an infinitely long dihedral corner. The three-dimensional, principal-plane, radar cross sections (RCS's) of the rectangular plate and of the finite-length dihedral corner reflector can be obtained from two-dimensional solutions using a simple truncation approximation [10]:

$$\sigma_{3\text{-}D} = \frac{2l^2}{\lambda} \sigma_{2\text{-}D} \tag{1}$$

where l is the finite length of the three-dimensional scatterer.

For three-dimensional scattering problems that cannot be simplified to the truncation of a two-dimensional geometry, such as oblique-incidence scattering in nonprincipal planes from a rectangular plate, the MEC is necessary because the UTD predicts scattered fields along the Keller cone of diffracted rays only. The MEC involves replacing a scatterer with nonphysical currents that radiate the same fields as the target scatters. These scattered fields are not restricted to the Keller cone; therefore, the MEC model can be used to predict nonprincipal-plane scattering.

Despite the versatility, easy applicability, and high accuracy of the UTD and the MEC for many scattering configurations, these methods do not account for all the possible scattering mechanisms that can

occur. Especially near and at grazing incidence, where multiple diffractions and corner diffractions seem to dominate, modifications to the present models are necessary to obtain more accurate results. A recent numerically formulated MEC accounts for scattering from corners over a limited range [11]. This report details the application of this diffraction model, including results and comparisons with experimental data.

Principal-plane diffraction from a perfectly conducting rectangular plate is a rather basic problem that is still an area of intense interest because of the ability to easily isolate the scattering mechanism between two parallel edges. The scattering mechanism near and at grazing incidence is of special interest. Some experimental trends remain unexplained despite the simplicity of the problem. This report presents the theoretical model and comparisons between theoretical and measured data.

Another area of current interest is that of coated targets and the modeling of a thin coating with a perfectly conducting backing. This report includes a shorted-transmission-line model for the metal-backed coating.

II. THEORY AND RESULTS

A. NONPRINCIPAL-PLANE SCATTERING FROM A RECTANGULAR PLATE

The MEC model of the rectangular plate for first-order diffraction terms assumes that the plate is electrically large so that interactions among the sides can be neglected and the plate can be approximately represented as four joined half planes. Each half plane is then replaced by the appropriate half-plane equivalent current. This model does not account for the joining of the planes at the corners, which results in discrepancies between theory and experiment near grazing incidence angles where corner diffraction terms are relatively significant in the scattering process. A focus of much research interest has been the formulation of a corner diffraction model. Using numerical curve fitting and comparisons with moment method (MM) results, Hansen [11] has formulated a corner diffraction model. Although this model is limited in its region of applicability, it appears to be a promising model.

The corner diffraction model is similar to the MEC in application. The following equivalent corner diffraction currents were formulated from numerical curve fitting:

SOFT POLARIZATION:

$$I_{\phi}(\theta',\phi') = \lambda\, e^{-j}\, [\, A(\theta',\phi')\ (\theta'-45^{\circ})^{2} + B(\phi')\ (\theta'-45^{\circ}) + C_{o}\,] \qquad (2)$$

where

$$A(\theta',\phi') = 0, \qquad \theta' < 45^\circ \text{ or } \phi' > 40^\circ$$

$$A(\theta',\phi') = A_o(40^\circ-\phi')^{1.5} \qquad \theta' \geq 45^\circ \text{ and } \phi' \leq 40^\circ$$

$$B(\phi') = B_o(90^\circ-\phi')^{1.5}$$

$$A_o = 1.00 * 10^{-6}$$

$$B_o = 4.40 * 10^{-6}$$

$$C_o = 1.70 * 10^{-1}$$

and

$$20^\circ \leq \phi' \leq 70^\circ, \qquad 0 \leq \theta' \leq 90^\circ$$

HARD POLARIZATION

$$I_\theta(\theta',\phi') = \lambda\, e^{j2.2}\, [\, A(\theta')\ (70^\circ-\phi')^2 + B(\theta')\ (70^\circ-\phi') + C(\theta')\,] \qquad (3)$$

where

$$A(\theta') = A_o(\theta'-25^\circ), \qquad \theta' \leq 55^\circ$$

$$A(\theta') = A_o(\theta'-25^\circ)\left\{\frac{\cos(\theta')}{\cos(55^\circ)}\right\}^{0.75} \qquad \theta' > 55^\circ$$

$$B(\theta') = B_o(90^\circ-\theta')$$

$$C(\theta') = C_o(90^\circ-\theta')$$

$$A_o = 1.26 * 10^{-6}$$

$$B_o = 3.48 * 10^{-5}$$

$$C_o = 8.75 * 10^{-4}$$

where, once again,

$$20^\circ \leq \phi' \leq 70^\circ, \qquad 0 \leq \theta' \leq 90^\circ$$

Each corner launches two current components, one along each of the adjoining edges. The fields radiated by these equivalent currents are found using the vector potential:

$$A(r) = \frac{\mu e^{-jkr}}{4\pi r} \int_{edge} I(\theta',\phi')\ \hat{t}\ e^{-jks'} e^{jk\hat{r}\cdot\hat{r}'}\ ds' \tag{4}$$

where

r = distance from the center of the plate (origin of the coordinate system) to the point of observation

$\hat{t}$ = unit vector tangent to the edge of interest

s' = distance from the corner of interest to the point of interest

$\hat{r}$ = unit vector from the origin toward the observation point

$\hat{r}'$ = unit vector from the origin toward the integration point

Finally, in the far field:

$$E_r \cong 0 \tag{5}$$

$$E_\theta \cong -j\omega A_\phi \tag{6}$$

$$E_\phi \cong -j\omega A_\theta \tag{7}$$

The integrals involved, for the plate geometry, simplify to a closed form. A total of eight integrals, two for each corner, must be evaluated.

The corner currents were formulated for a limited region of incidence:

$$0^\circ \leq \theta' \leq 90^\circ \qquad 20^\circ \leq \phi' \leq 70^\circ$$

Symmetry considerations do not allow the extension of this model to other incidence angles, contrary to what was reported previously [12], because of the interference of higher-order mechanisms, such as scattering among sides. For those angles not included in the present

corner diffraction model, the corner diffraction terms must be set to 0. Results for this model are in Figs. 2 - 5 for the geometry of Fig. 1. The agreement between the theoretical and experimental data is better for the soft polarization than for the hard polarization. This indicates that higher-order scattering mechanisms are more dominant for the hard polarization than for the soft polarization. Also, the agreement between theory and experiment is better for a tilt angle of 30° than for a tilt angle of 45°. This is probably due to the dominance of corner scattering at the 45° tilt angle. The biggest disagreement, especially for the hard polarization, is in the outermost two lobes. We are trying to isolate the mechanisms that contribute to the formation of these lobes so that we can more closely and carefully account for them.

The present theoretical model contains only first-order diffraction mechanisms and terms to account for the scattering from one of the four corners which is closest to the source. Accounting for the scattering from only one corner results in a marked improvement over the results from the first-order model, which does not account for any corner diffraction, reported in [3]. A model to account for the corner scattering from all corners is not yet available due to the limited range of the MEC model of (2) and (3). These limits are imposed because of the inability to isolate corner scattering terms at other incidence angles.

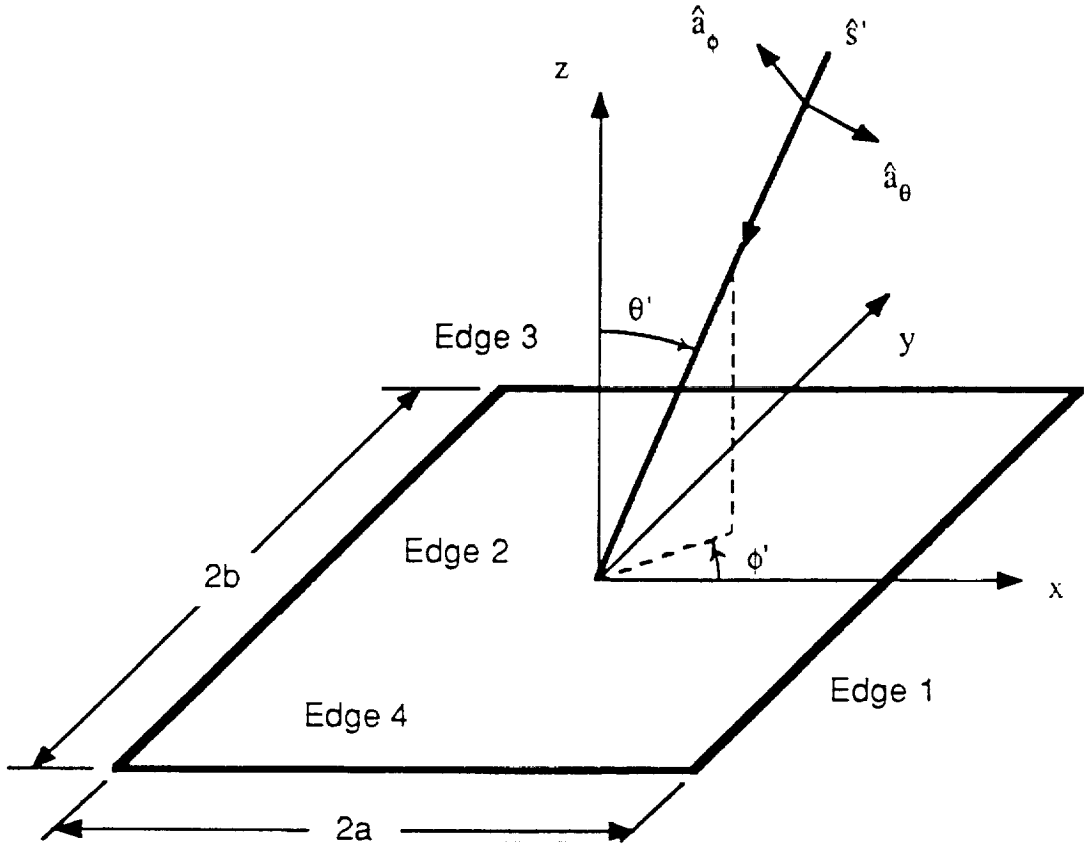

Fig. 1. Rectangular plate geometry.

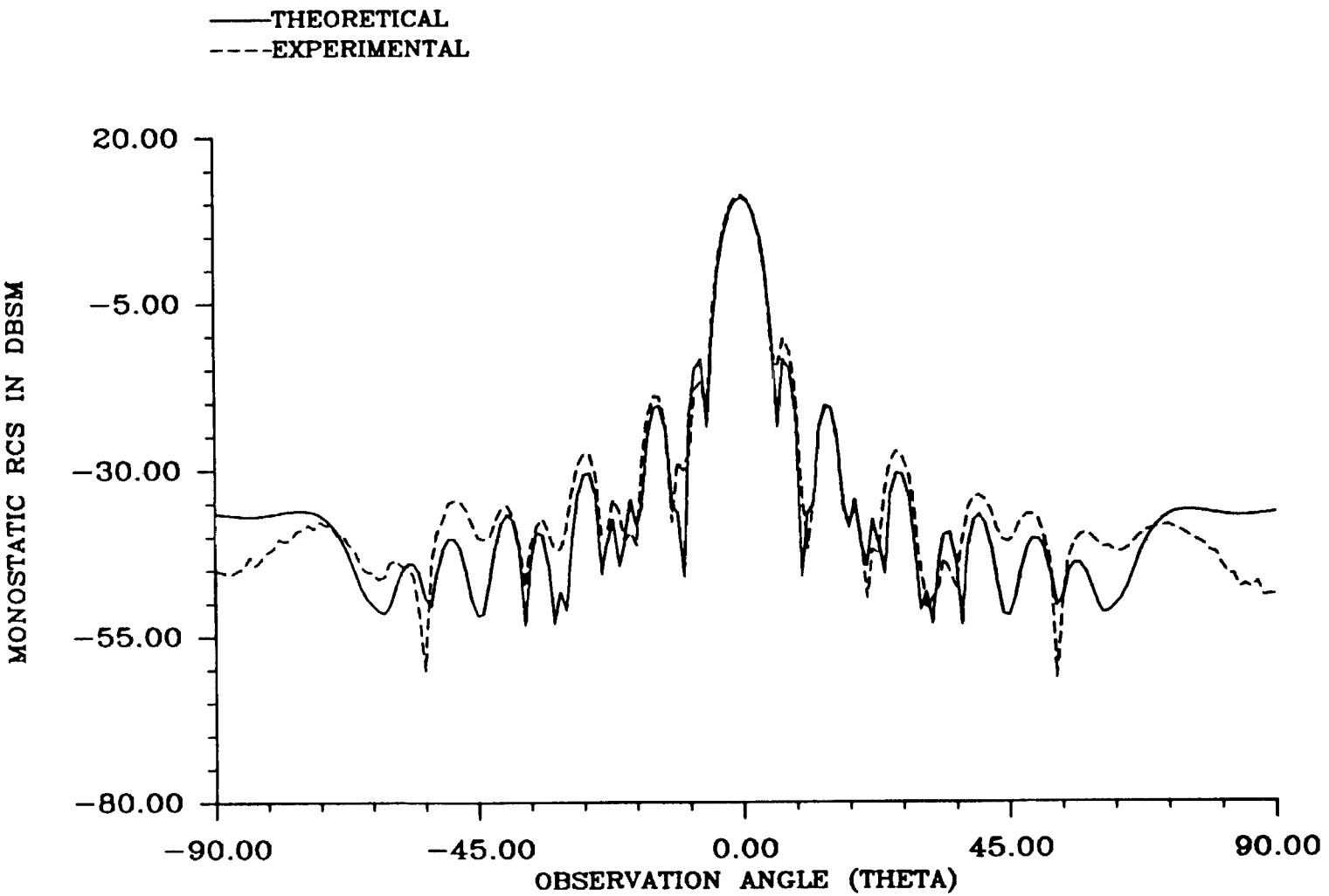

Fig. 2. Monostatic RCS of a square plate (soft polarization, $2a = 2b = 17.18$ cm, $f = 10$ GHz, $\phi' = 30^{\circ}$).

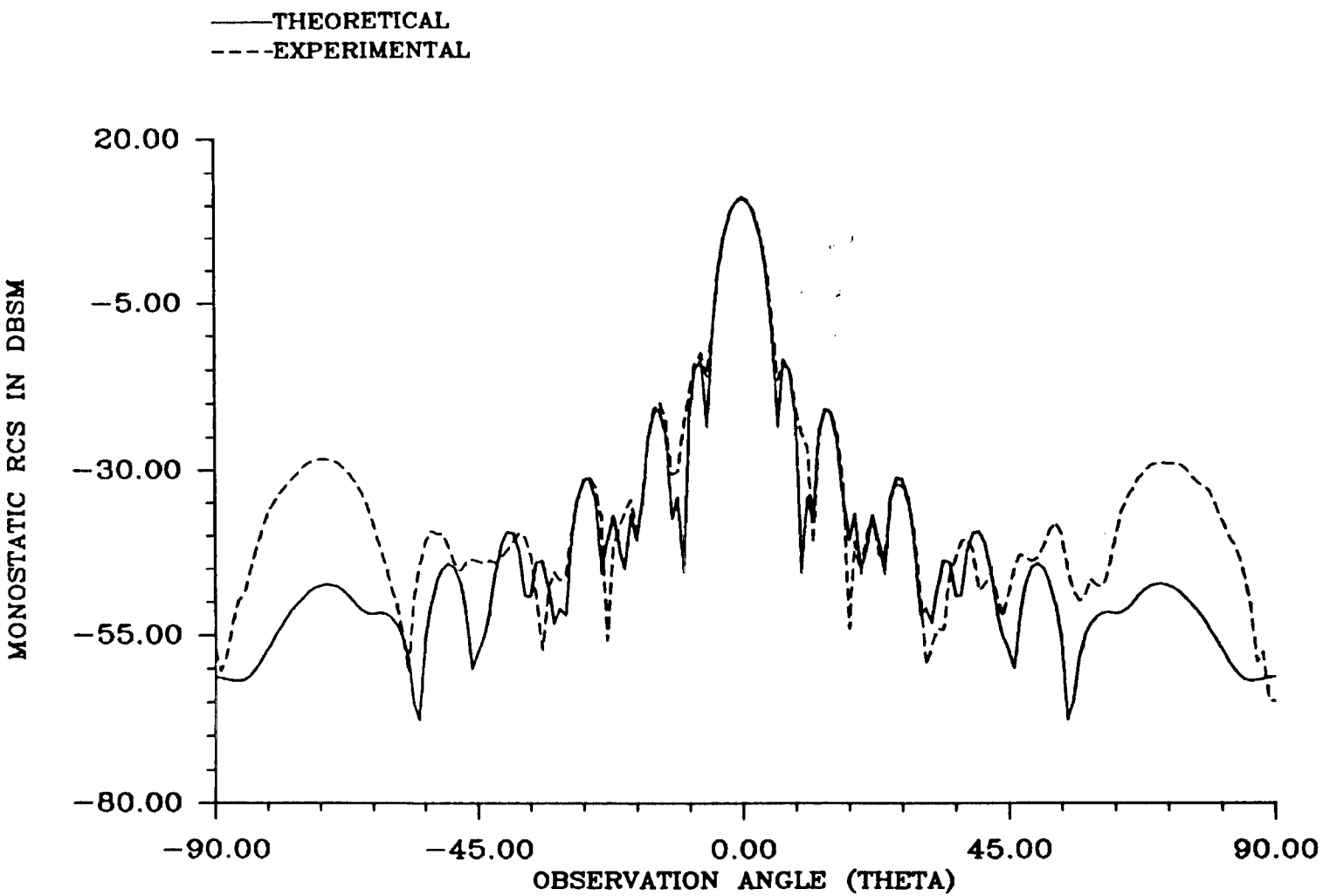

Fig. 3. Monostatic RCS of a square plate (hard polarization, $2a = 2b = 17.18$ cm, $f = 10$ GHz, $\phi' = 30^{\circ}$).

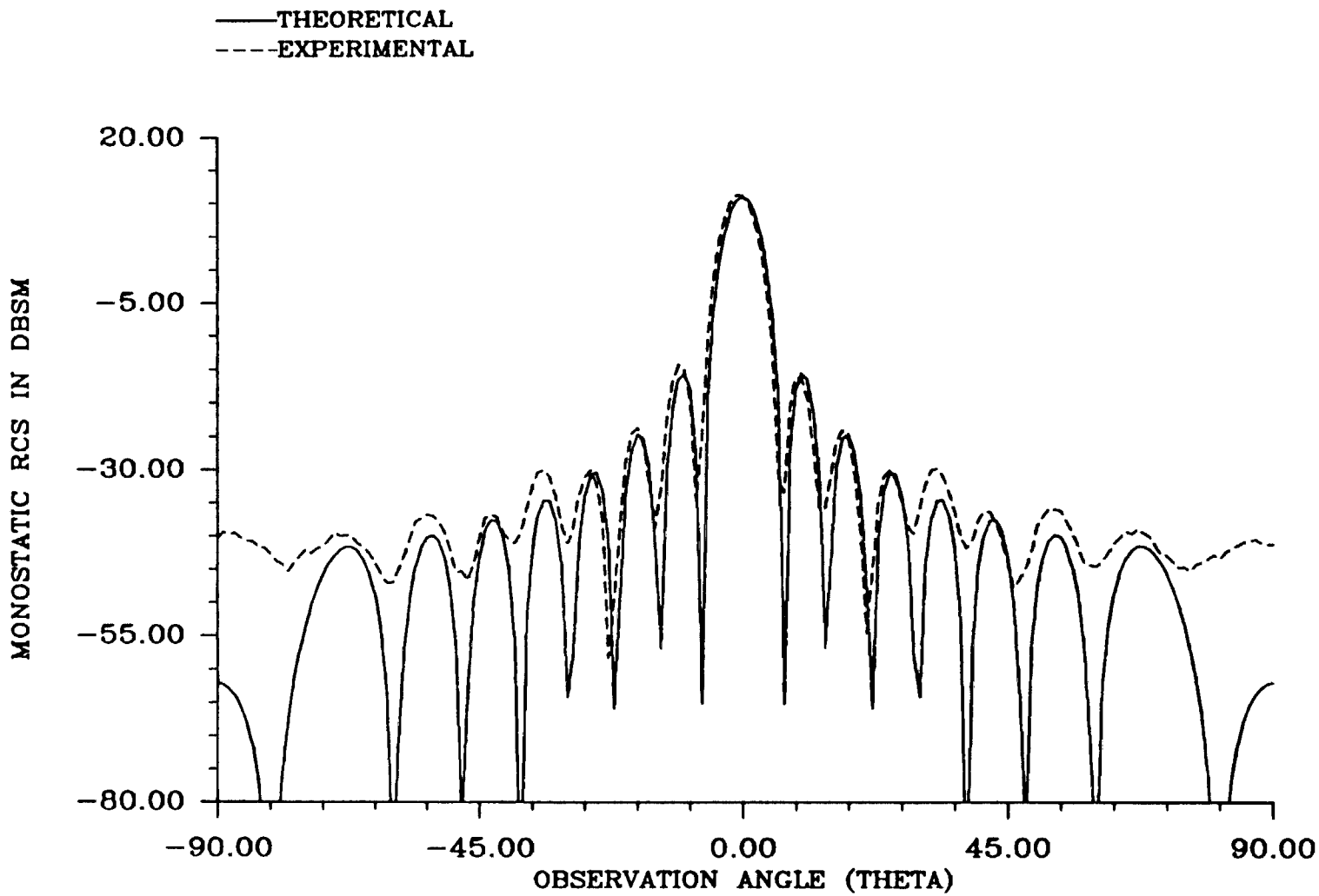

Fig. 4. Monostatic RCS of a square plate (soft polarization, $2a = 2b = 17.18$ cm, $f = 10$ GHz, $\phi' = 45^{\circ}$).

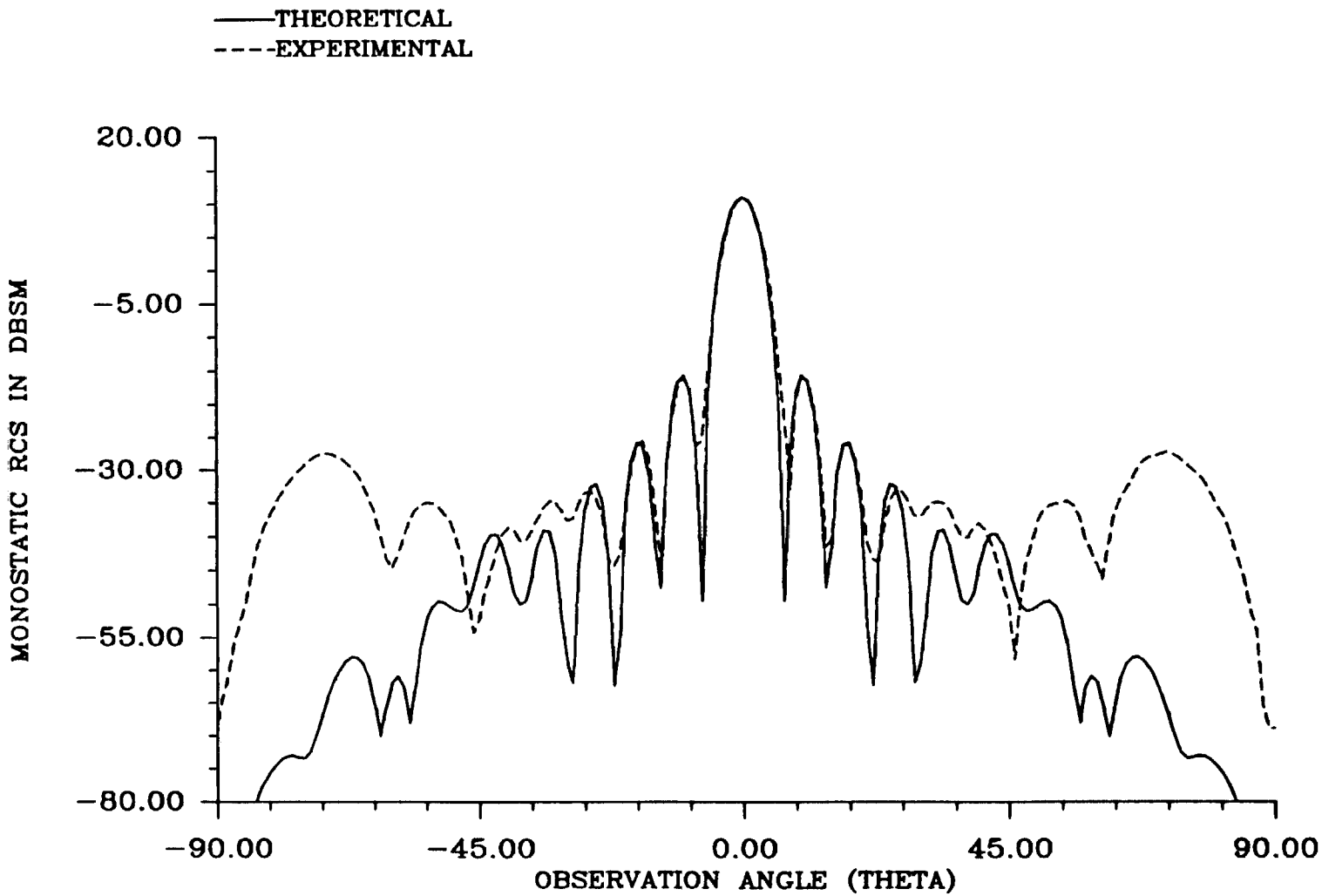

Fig. 5. Monostatic RCS of a square plate (hard polarization, $2a = 2b = 17.18$ cm, $f = 10$ GHz, $\phi' = 45^{\circ}$).

B. PRINCIPAL-PLANE SCATTERING FROM A PERFECTLY CONDUCTING RECTANGULAR PLATE

The principal-plane scattering from a rectangular plate can be modeled using an infinite strip and the truncation equation of (1). Because this is simply a two-dimensional problem, the UTD can be used quite accurately for the perfectly conducting plate. Near grazing incidence the UTD theoretically fails because of the existence of overlapping transition regions in which the UTD is not applicable; however, for monostatic backscattering the UTD actually produces quite accurate results.

The geometry of interest is shown in Fig. 6. According to the UTD, diffracted fields can be represented as:

$$\underline{E}^d(s) = \underline{E}^i(Q_D) \circ \tilde{D}\, A(s)\, e^{-jks} \tag{8}$$

where

$\underline{E}^i(Q_D)$ = the incident field at the point of diffraction

$\tilde{D}$ = the dyadic diffraction coefficient

$A(s)$ = the amplitude spreading factor

e^{-jks} = the phase factor

s = the distance from the point of diffraction to the observation point

There are two different forms of D, the diffraction coefficient — the original Geometrical Theory of Diffraction (GTD) form [13] and the UTD form [5]. In this formulation, the GTD coefficient is used for first-order diffractions and the UTD coefficient for higher-order

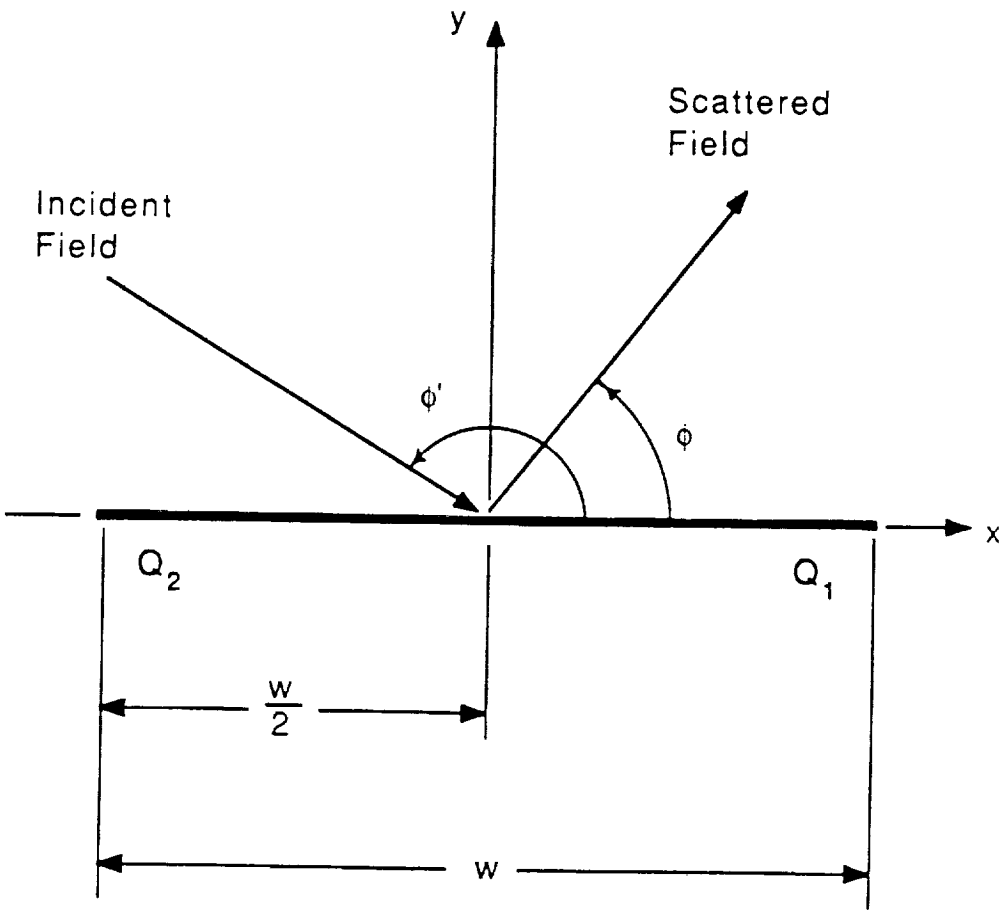

Fig. 6. Strip/plate geometry.

diffractions. The GTD coefficients for principal-plane, monostatic scattering from a half-plane are:

GTD COEFFICIENTS

SOFT POLARIZATION

$$D_s = \frac{e^{-j(\pi/4)}}{2\sqrt{2\pi k}} \left\{ -1 + \frac{1}{\cos(\phi')} \right\} \tag{9}$$

HARD POLARIZATION

$$D_h = \frac{e^{-j(\pi/4)}}{2\sqrt{2\pi k}} \left\{ -1 - \frac{1}{\cos(\phi')} \right\} \tag{10}$$

The UTD coefficients are more complicated, involving cotangent functions and Fresnel transition functions. They are explicitly defined in [5] and throughout the literature, and they will not be repeated here. Subroutines for calculating the coefficients are available in [14] and [15]. The crucial parameters that must be specified are the polarization; the distance between the source and diffraction point, d; the incidence angle, ϕ'; and the diffraction angle, ϕ. The diffraction coefficient will thus be designated in the form, D(polarization,d,ϕ',ϕ).

Using the standard definition of the two-dimensional echo width [15], the echo width for principal-plane, monostatic scattering from a strip of width, w, accounting for first-order diffractions only is:

$$\sigma_{2\text{-}D} = (k)^{-1} \left\{ \left[\cos(kw \cos\phi') \right]^2 + \left[\frac{\sin(kw \cos\phi')}{\cos\phi'} \right]^2 \right\} \tag{11}$$

Eq. (1) can be used to find the three-dimensional RCS of the corresponding rectangular plate.

For the soft polarization case, higher-order diffractions do not exist; however, slope diffraction terms can be included using the theory outlined in [15]. Subroutines for calculating the slope diffraction coefficients, DS(polarization,d,ϕ',ϕ), are included in [15]. Omitting the details, the final slope diffracted field for soft polarization is:

$$E_{ds} = -jk^{-1}\frac{e^{-jk\rho}}{\sqrt{\rho}}\left\{\frac{\partial}{\partial n}[E^i(Q_1)]\ DS_1\ e^{jk(w/2)\cos\phi'} + \frac{\partial}{\partial n}[E^i(Q_2)]\ DS_2\ e^{-jk(w/2)\cos\phi'}\right\} \tag{12}$$

where

$$\frac{\partial}{\partial n}[E^i(Q_1)] \cong \left(\frac{180}{w\pi}\right)\left(E_o\ e^{-jk(w/2)\cos\phi'}\right)\frac{e^{-jkw}}{\sqrt{\rho}}\ D_{21}^s$$

$$\frac{\partial}{\partial n}[E^i(Q_2)] \cong \left(\frac{180}{w\pi}\right)\left(E_o\ e^{jk(w/2)\cos\phi'}\right)\frac{e^{-jkw}}{\sqrt{\rho}}\ D_{12}^s$$

$$D_{21}^s = D(soft,w,1^\circ,180^\circ-\phi')$$

$$D_{12}^s = D(soft,w,1^\circ,\phi')$$

$$DS_1 = DS(soft,w,0^\circ,180^\circ-\phi')$$

$$DS_2 = DS(soft,w,0^\circ,\phi')$$

For the hard polarization case, higher-order diffractions play a significant role in the total RCS. Even third-order and fourth-order terms are relatively large at incidence angles away from normal

incidence. Using (8) and the UTD coefficients, the general form of the nth-order diffraction term for the infinite strip is:

$$E^{nth} = -E_o \frac{e^{-jk\rho}}{\sqrt{k\rho}} \sqrt{\frac{k}{w^{n-1}}} \left\{ e^{-jk(w/2)((-1)^{(n-1)}\cos\phi')} \times e^{-jk(w/2)(\cos\phi' + 2(n-1))} D(\text{hard}, w, \phi', 0^\circ) \right\} \times \left\{ \left(D(\text{hard}, w, 0^\circ, 0^\circ) \right)^{n-2} D\left(\text{hard}, w, 0^\circ, \begin{matrix} 180^\circ - \phi' & (n=\text{even}) \\ \text{or } \phi' & (n=\text{odd}) \end{matrix} \right) \right\} \tag{13}$$

$$+ e^{jk(w/2)((-1)^{(n-1)}\cos\phi' + \cos\phi' - 2(n-1))} D(\text{hard}, w, 180^\circ - \phi', 0^\circ) \times \left\{ \left(D(\text{hard}, w, 0^\circ, 0^\circ) \right)^{n-2} D\left(\text{hard}, w, 0^\circ, \begin{matrix} 180^\circ - \phi' & (n=\text{odd}) \\ \text{or } \phi' & (n=\text{even}) \end{matrix} \right) \right\}$$

Using (1) and the standard definition of the two-dimensional echo width, the three-dimensional RCS for the corresponding rectangular plate is obtained.

Comparisons between theory and measurements are included in Figs. 7 - 10. The soft polarization model includes the first-order and slope-diffraction terms and the hard polarization model includes up to fourth-order terms. The agreement between theory and experiment is very good, even for diffraction distances as small as $\lambda/2$. The small errors near and at grazing incidence are probably due to the approximation of (1). There appears to be a scattering mechanism associated with the two edges of the plate parallel to the plane of diffraction for which the UTD does not account.

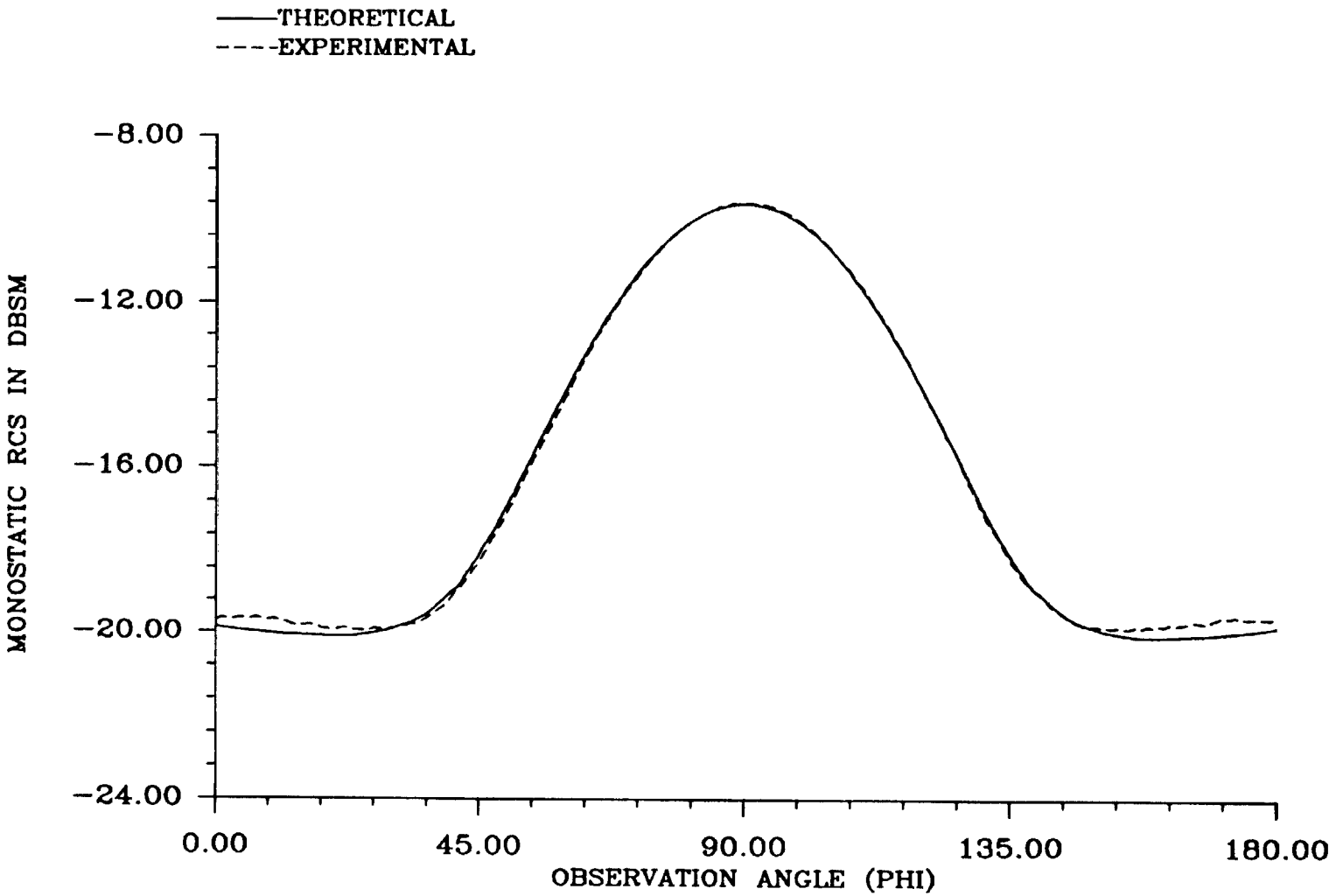

Fig. 7. Monostatic RCS of a rectangular plate ($w = \lambda/2$, $l = 6\lambda$, principal plane, soft polarization).

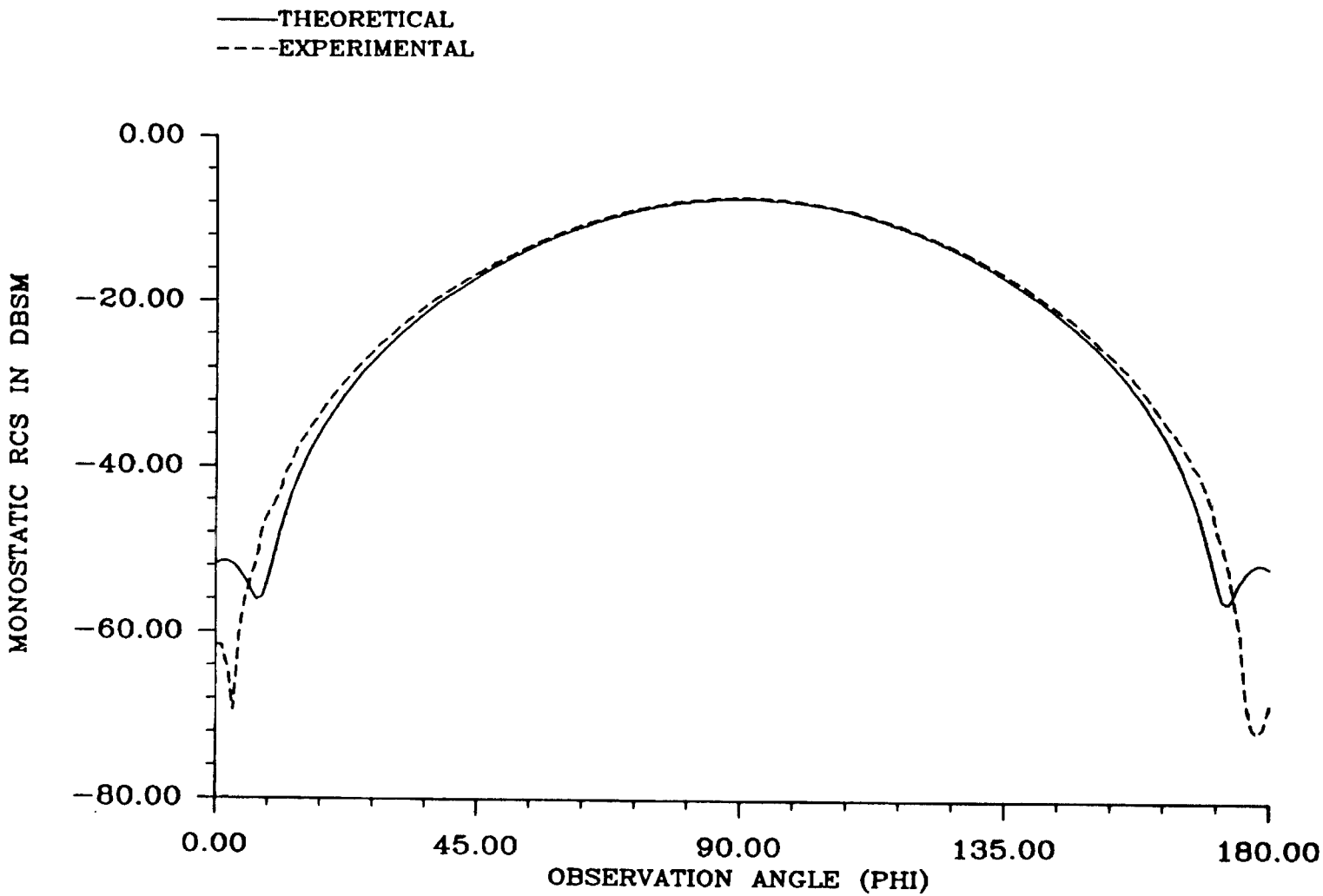

Fig. 8. Monostatic RCS of a rectangular plate ($w = \lambda/2$, $l = 6\lambda$, principal plane, hard polarization).

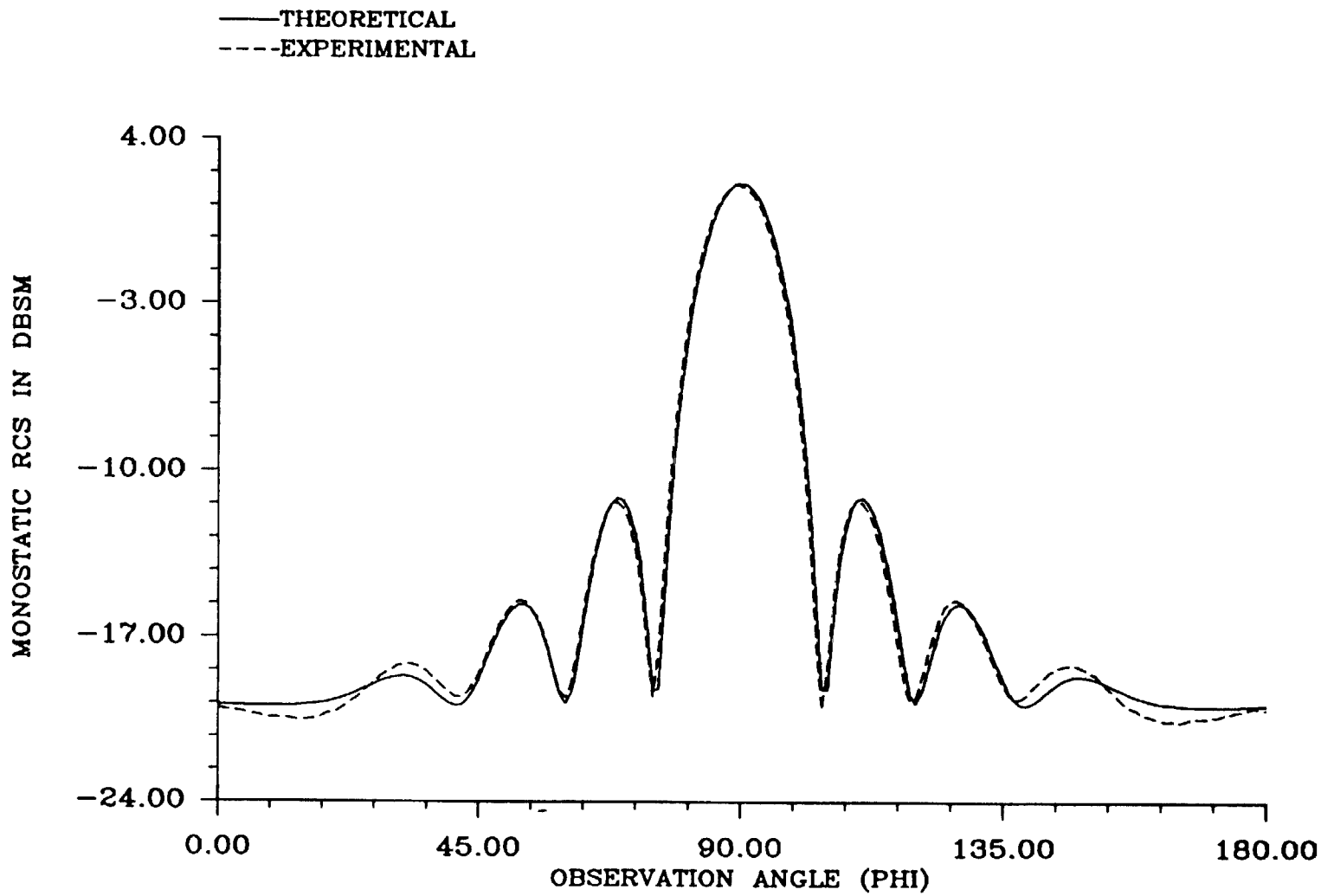

Fig. 9. Monostatic RCS of a rectangular plate ($w = 2\lambda$, $l = 6\lambda$, principal plane, soft polarization).

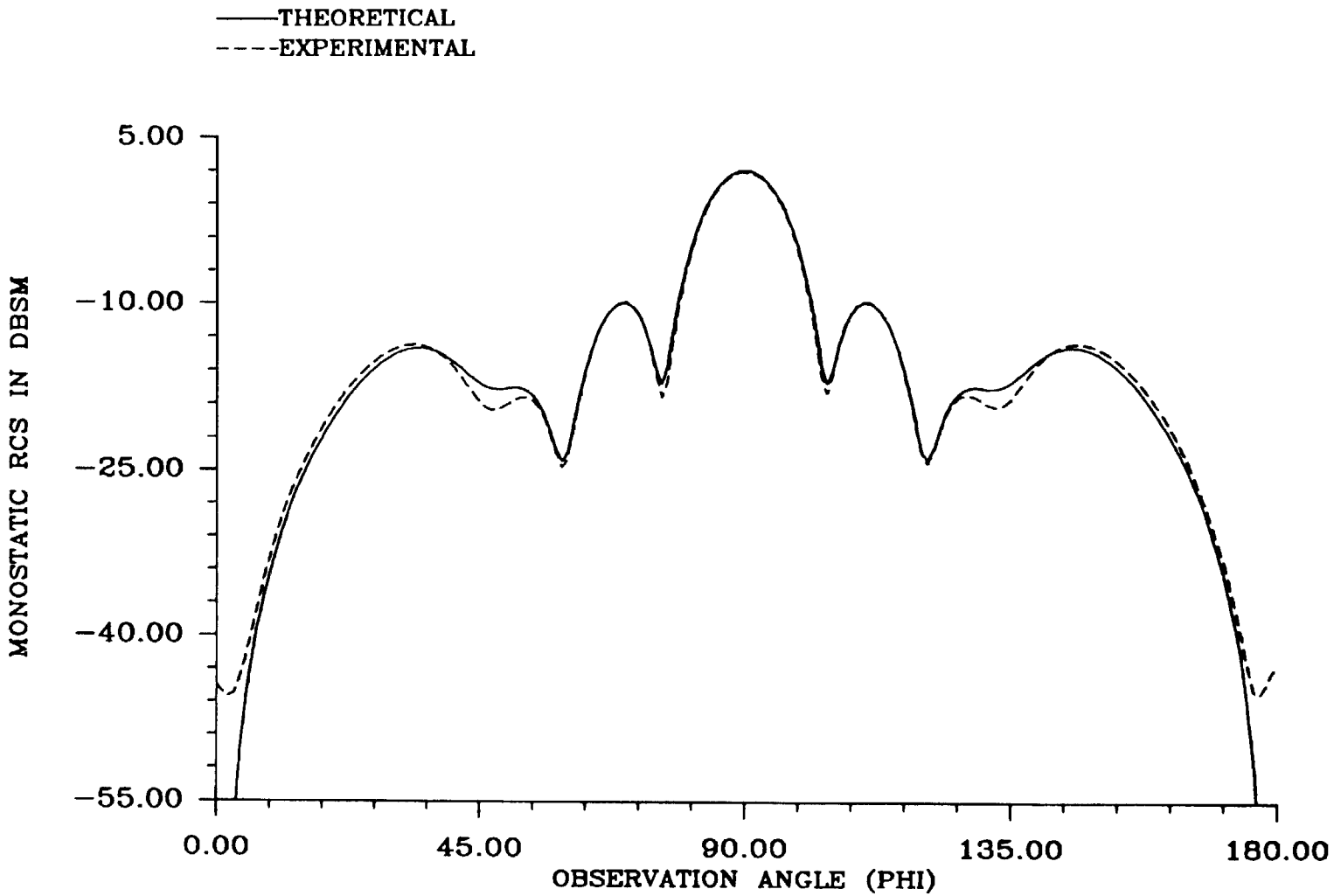

Fig. 10. Monostatic RCS of a rectangular plate ($w = 2\lambda$, $l = 6\lambda$, principal plane, hard polarization).

C. PRINCIPAL-PLANE SCATTERING FROM A COATED, RECTANGULAR PLATE

The principal-plane RCS of the coated, rectangular plate of Fig. 11 is formulated in the same manner as the principal-plane RCS of the perfectly conducting rectangular plate except that the diffraction coefficient is the impedance-wedge diffraction coefficient formulated by Griesser and Balanis [16]. In order to use this diffraction coefficient, the equivalent impedance of the coated conductor must be found. The impedance boundary condition will be used so that the equivalent impedance normalized to the impedance of free space is:

$$\eta_{eq} = j\eta \tan(kt \sin(\phi_t)) \tag{14}$$

where

$\eta = \sqrt{\mu_c/\varepsilon_c}$

$k = \omega \sqrt{\mu\varepsilon}$

t = the coating thickness

μ_c, ε_c = the relative permeability and relative permittivity of the coating

μ, ε = the permeability and permittivity of the coating

ϕ_t = the angle of the transmitted ray as measured from the surface of the coating

Assuming cylindrical-wave incidence and plane-wave diffraction and using, the two-dimensional echo width for an infinite, coated strip is:

$$\sigma_{2\text{-}D} = 2\pi\rho' \left\{ D_1 \frac{e^{-jk\rho_1'}}{\sqrt{\rho_1'}} e^{-j(kw/2)\cos\phi'} \right. \tag{15}$$

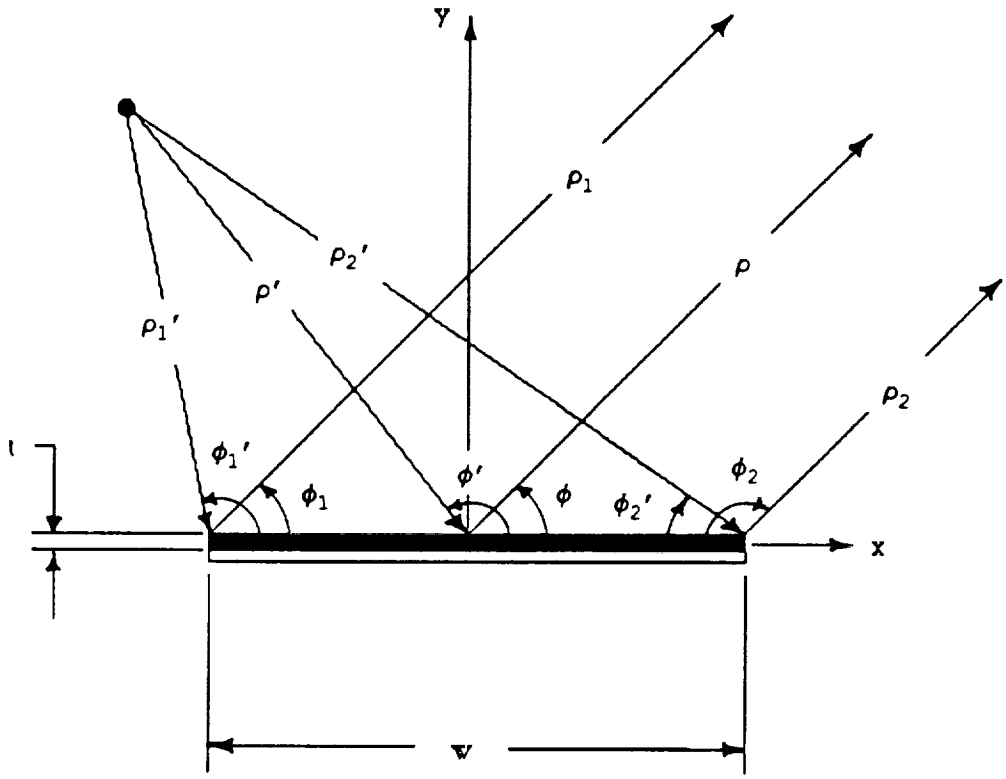

Fig. 11. Coated strip/plate geometry.

$$+ \quad D_2 \frac{e^{-jk\rho_2'}}{\sqrt{\rho_2'}} e^{-j(kw/2)\cos\phi'} \Bigg\}^2$$

where

$$D_1 = DC(\text{polarization}, \phi_1', \phi_1, \frac{\rho_1'}{2}, \theta_o, \theta_n)$$

$$D_2 = DC(\text{polarization}, \phi_2', \phi_2, \frac{\rho_2'}{2}, \theta_o, \theta_n)$$

$DC(\text{polarization}, \psi', \psi, d, \theta_o, \theta_n)$ is the diffraction coefficient for an impedance wedge presented in [16]. ψ' and ψ are the angles of incidence and diffraction, respectively. θ_o and θ_n are the Brewster angles associated with the equivalent impedance of the surface of interest:

SOFT POLARIZATION

$$\theta_o = \sin^{-1}(1/\eta_o) \tag{16}$$

$$\theta_n = \sin^{-1}(1/\eta_n) \tag{17}$$

HARD POLARIZATION

$$\theta_o = \sin^{-1}(\eta_o) \tag{18}$$

$$\theta_n = \sin^{-1}(\eta_n) \tag{19}$$

where

η_o = surface impedance of face "o", normalized with respect to the free-space impedance as in (8)

η_n = surface impedance of face "n", normalized with respect to the free-space impedance as in (8)

Comparisons between the theoretical model and experimental data were included in the last report [4]. The theoretical model included no higher-order terms, such as surface wave terms and second-order and third-order diffraction terms. Consequently there was a great deal of

discrepancy between the theoretical and the experimental results. A more sophisticated model is currently being formulated. Results will be included in the next report.

III. FUTURE WORK

After examining several basic plate geometries, it is obvious that, despite the relative maturity of high-frequency scattering prediction methods, there remain many scattering mechanisms that are, as of yet, unexplained. Future work will concentrate on developing and improving high-frequency scattering models so that all the observed mechanisms may be explained and predicted. Specific work includes improving the corner diffraction model for nonprincipal-plane prediction, accounting for the influence of all four edges of the plate in principal-plane scattering, and improving the model for coated plates. The coated dihedral corner reflector model will also be revised and improved to more effectively account for the finite-thickness coating.

Another objective that will be pursued in the next reporting period is to experimentally isolate the scattering mechanisms on the rectangular plate. This will be accomplished by performing an extensive set of measurements of the plate RCS with various prominent scattering points covered with absorbing material. For example, to

isolate the scattering from the corner nearest the source, the scattering from the other three corners will be suppressed by covering them with absorbing material. Diffractions among edges will also be studied in this manner. This experimental work will pinpoint important diffraction mechanisms to add to the present theoretical model of the plate.

IV. REFERENCES

[1] C. A. Balanis, L. A. Polka, and K. Liu, "Nonprincipal-plane scattering from rectangular plates and pattern control of horn antennas," Semiannual Report, Grant No. NAG-1-562, National Aeronautics and Space Administration, Langley Research Center, Hampton, VA, Jan. 31, 1990.

[2] C. A. Balanis, L. A. Polka, and K. Liu, "Nonprincipal-plane scattering from flat plates — second-order and corner diffraction and pattern control of horn antennas," Semiannual Report, Grant No. NAG-1-562, National Aeronautics and Space Administration, Langley Research Center, Hampton, VA, Jul. 31, 1989.

[3] C. A. Balanis, L. A. Polka, and K. Liu, "Nonprincipal plane scattering of flat plates and pattern control of horn antennas," Semiannual Report, Grant No. NAG-1-562, National Aeronautics and Space Administration, Langley REsearch Center, Hampton, VA, Jan. 31, 1989.

[4] C. A. Balanis, L. A. Polka, and K. Liu, "Scattering from coated structures and antenna pattern control using impedance surfaces," Semiannual Report, Grant No. NAG-1-562, National Aeronautics and Space Administration, Langley Research Center, Hampton, VA, Jul. 31, 1990.

[5] R. G. Kouyoumjian and P. H. Pathak, "A uniform geometrical theory of diffraction for an edge in a perfectly conducting surface," *Proc. IEEE*, vol. 62, pp. 1448-1461, Nov. 1974.

[6] A. Michaeli, "Equivalent edge currents for arbitrary aspects of observation," *IEEE Trans. Antennas Propagat.*, vol. AP-32, pp. 252-258, Mar. 1984.

[7] ——, "Elimination of infinities in equivalent edge currents, part II: physical optics components," *IEEE Trans. Antennas Propagat.*, vol. AP-34, pp. 1034-1037, Aug. 1986.

[8] ——, "Elimination of infinities in equivalent edge currents, part I: fringe current components," *IEEE Trans. Antennas Propagat.*, vol. AP-34, pp. 912-918, July 1986.

[9] ——, "Equivalent currents for second-order diffraction by the edges of perfectly conducting polygonal surfaces," *IEEE Trans. Antennas Propagat.*, vol. AP-35, pp. 183-190, Feb. 1987.

[10] R. A. Ross, "Radar cross section of rectangular flat plates as a function of aspect angle," *IEEE Trans. Antennas Propagat.* vol. AP-14, pp. 329-335, May 1966.

[11] T. B. Hansen, "An investigation of the currents due to right-angled corners of flat plates," Technical Report, Electromagnetics Institute, Technical University of Denmark, Jan. 1990.

[12] C. A. Balanis and L. A. Polka, "RCS prediction for oblique incidence angles and coated structures," Research Proposal, Grant No. NAG-1-562, National Aeronautics and Space Administration, Langley Research Center, Hampton, VA, Nov. 1990.

[13] J. B. Keller, "Geometrical theory of diffraction, *J. Opt. Soc. Amer.*, vol. 52, pp. 116-130, Feb. 1962.

[14] C. A. Balanis, *Antenna Theory: Analysis and Design*. New York: Harper and Row Publishers, Inc., 1982.

[15] C. A. Balanis, *Advanced Engineering Electromagnetics*. New York: John Wiley & Sons, 1989.

[16] T. Griesser and C. A. Balanis, "Reflections, diffractions, and surface waves for an interior impedance wedge of arbitrary angle," *IEEE Trans. Antennas Propagat.*, vol. AP-37, pp. 927-935, July 1988.